Published in final edited form as:
Magn Reson Imaging. 2012 April ; 30(3): 361–370. doi:10.1016/j.mri.2011.10.004.

Depth and orientational dependencies of MRI T_2 and $T_{1\rho}$ sensitivities towards trypsin degradation and Gd-DPTA^{2-} presence in articular cartilage at microscopic resolution

Nian Wang, PhD and **Yang Xia, PhD***
Department of Physics and Center for Biomedical Research, Oakland University, Rochester, MI 48309

Abstract

Depth and orientational dependencies of microscopic MRI T_2 and $T_{1\rho}$ sensitivities were studied in native and trypsin-degraded articular cartilage, before and after being soaked in 1 mM Gd-DTPA^{2-} solution. When the cartilage surface was perpendicular to B_0, a typical laminar appearance was visible in T_2 weighted images but not in $T_{1\rho}$ weighted images, especially when the spin-lock field was high (2 kHz). At the magic angle (55°) orientation, neither T_2 nor $T_{1\rho}$ weighted image had a laminar appearance. Trypsin degradation caused a depth and orientational dependent T_2 increase (4–64%) and a more uniform $T_{1\rho}$ increase at a sufficiently high spin-lock field (55–81%). The presence of the Gd ions caused both T_2 and $T_{1\rho}$ to decrease significantly in the degraded tissue (6–38% and 44–49% respectively) but less notably in the native tissue (5–10% and 16–28% respectively). A quantity *Sensitivity* was introduced that combined both the percentage change and the absolute change in the relaxation analysis. An MRI experimental protocol based on two $T_{1\rho}$ measurements (without and with the presence of the Gd ions) was proposed to be a new imaging marker for cartilage degradation.

Keywords

T_2; $T_{1\rho}$; MRI; cartilage; proteoglycan; magic angle; anisotropy; spin lock

Introduction

Articular cartilage, which is a thin layer of soft tissue covering the ends of bone in joint to distribute external loading, consists mainly of structured collagen fibrils, negatively charged proteoglycans (PG) and water molecules in its extracellular matrix (1,2). Since the orientation of the collagen fibrils in articular cartilage is depth dependent, the total depth (thickness) of articular cartilage is commonly subdivided based on the local fibril orientation into multiple structural zones, such as the superficial zone at the top surface (SZ), the transitional zone (TZ) in the middle, and the radial zone (RZ) that interfaces with the underlining bone. The role of negatively charged PG molecules is to generate a volumetric tension inside the tissue by absorbing water. A reduction of PG in cartilage is an early event

***Corresponding Author and Address**, Yang Xia, PhD, Department of Physics, Oakland University, Rochester, Michigan 48309, USA, Phone: (248) 370-3420, Fax: (248) 370-3408, xia@oakland.edu.

in the gradual process of tissue degradation, which will eventually lead to clinical diseases such as osteoarthritis (OA) that affects over 20 million people in the United States (3).

Magnetic resonance imaging (MRI) is a sensitive diagnostic technique suitable for the noninvasive assessment of soft tissue such as articular cartilage. Conventional (i.e., intensity based) MRI, however, does not have the sensitivity towards the subtle changes associated with the early stage of cartilage lesions (4–6). A number of quantitative techniques have been developed in MRI to better evaluate the structural and concentrational changes associated with the tissue degradation, including three MRI techniques that utilize the relaxation time measurement: the value and anisotropy of T_2 relaxation (7–9), the gadolinium-enhanced T_1 relaxation (dGEMRIC) (10–14), and $T_{1\rho}$ relaxation (spin-lattice relaxation in the rotating frame) (15–18).

The transverse relaxation time T_2 is sensitive to the anisotropic motion of water molecules mediated by the collagen orientation via dipolar interaction (7). This T_2 anisotropy can cause articular cartilage to have a depth-dependent laminar appearance in MRI when the normal axis of cartilage surface is in parallel with the external magnetic field B_0 (7,19–21). When the normal axis is about 55° to B_0, the minimization of the dipolar interaction causes the disappearing of the laminar appearance and the increased cartilage intensity, an effect known as the “magic-angle effect” in the literature of cartilage MRI (8,9,21).

The longitudinal relaxation time T_1, in contrast, is insensitive to the anisotropic motion of water molecules mediated by the collagen orientation (7). Hence T_1 in articular cartilage is nearly isotropic and largely depth-independent (7). The usefulness of T_1 measurement in cartilage MRI was pioneered by the development of the clinical procedure (dGEMRIC, delayed Gadolinium Enhanced Magnetic Resonance Imaging of Cartilage) (10,22), which, in principle, images patient/specimen twice before/after it is injected with or immersed in a solution of a paramagnetic contrast agent, Gd-DTPA^{2-}. Since gadolinium ions shorten the T_1 relaxation and distribute in an inverse relation to the concentration of the negatively charged PG molecules in cartilage, both before and after injection/immersion images can be used to calculate the PG concentration in cartilage.

The spin-lattice relaxation time in the rotating frame $T_{1\rho}$ is also sensitive to the slow motional interactions between water and macromolecules (proteins) in biological tissues and has been used in recent years in cartilage imaging (16,23–25). Since $T_{1\rho}$ is less sensitive to the local fibril orientation, $T_{1\rho}$ has less anisotropy in articular cartilage MRI, which is a welcome feature in human MRI where the specimen orientation cannot be adjusted easily. A unique feature of $T_{1\rho}$ is the dependency of its values on the strength of the spin-lock field (the rf field that locks the magnetization in the transverse plane), a phenomenon termed $T_{1\rho}$ dispersion (26).

This microscopic imaging project concerns the depth and orientational dependencies of both T_2 and $T_{1\rho}$ sensitivities in cartilage MRI, in the absence and presence of the contrast agent Gd-DTPA^{2-} in the tissue. The dependency of T_2 in the presence of (gadolinium) Gd has been discussed in several studies (27–30), but rarely the dependency of $T_{1\rho}$ in the presence of Gd ions. In addition, the influence of the specimen orientation in the magnetic field on T_2 and $T_{1\rho}$ measurements has not been adequately investigated. In this high-resolution imaging project, the sensitivities of T_2 and $T_{1\rho}$ were studied at microscopic resolution (13 μm transverse resolution) in native and trypsin-degraded articular cartilage without and with the presence of Gd ions in the tissue. The influence of the specimen orientation in the magnet and the dependency of $T_{1\rho}$ on the strength of the spin-lock field were both being considered.

Materials and Methods

Cartilage Specimens

Canine humeral heads were harvested shortly after the sacrifice of three mature (1–2 years old) and musculoskeletally healthy dogs that were used for unrelated biomedical research (ongoing for more than the last 10 years). For each of the three dogs, two adjacent cartilage-bone blocks (about 1.8×1.5×6 mm^3) were harvested from the central part of one humeral head. The specimens were first imaged by the same μMRI protocols as their own controls. After the initial MRI, one specimen was immersed in 1 mM Gd-$DTPA^{2-}$ (Magnevist, Berlex, NJ) solution in saline with 1% protease inhibitor (Sigma, Missouri) for more than 8 hours before the second MRI experiment (13). The other specimen in the pair was first soaked in 0.1 mg/ml trypsin (Sigma, Missouri) solution for more than 8 hours to deplete proteoglycans (31) and then soaked in fresh saline with 1% protease inhibitor to remove excess trypsin before repeating the MRI. After repeating the MRI, this PG-depleted specimen was immersed in the Gd-$DTPA^{2-}$ saline and subsequently imaged using the same protocol for the third time. These experiments were repeated with four more cartilage blocks from two other dogs; the results were nearly identical (within the error range).

Microscopic MRI (μMRI) Protocols

All μMRI experiments were performed at room temperature on a Bruker AVANCE–300 NMR spectrometer equipped with a 7 Tesla/89 mm vertical-bore superconducting magnet and microimaging accessory (Bruker Instrument, Billerica, MA). A homemade 3 mm coil was used in the μMRI experiments, which had a 90° hard pulse of 5 μs. Quantitative T_2 experiments were performed using a CPMG magnetization-prepared T_2 imaging sequence (32). The $T_{1\rho}$ imaging sequence preceded with a 90° hard pulse followed by a spin-lock pulse. The strengths of the spin-lock field were 0.5 kHz and 2 kHz, which were calibrated by the strength of the 90° pulse.

The μMRI experiments were carried out with an acquisition matrix of 256×128 (13×26 μm pixel resolution) and a slice thickness of 1 mm. The repetition time TR was 2 s for the specimens without Gd-$DTPA^{2-}$ immersion and 0.8 s for the specimens soaked in Gd-$DTPA^{2-}$ solution. The echo spacing in the CPMG T_2-weighting segment was 1 ms and the number of echoes were 2, 4, 10, 30, 60 when the cartilage surface was perpendicular to the static magnetic field and 2, 14, 36, 60, 120 at the magic angle, respectively, which resulted in five T2-weighted images for each tissue orientation (at 0°: the effective contrast TEs = 2, 4, 10, 30, 60ms; at 55°: the effective contrast TEs = 2, 14, 36, 60, 120 ms). The lengths of the spin-locking pulse were 2, 6, 12, 40, 80 ms when the cartilage surface was perpendicular to the static magnetic field and 2, 18, 40, 80, 140 ms at the magic angle, respectively.

The 2D $T_{1\rho}$ images were calculated pixel-by-pixel by an expression: $Sig(TSL) = Sig_0\exp(-TSL/T_{1\rho}) + K$, where *Sig* was the signal intensity of the observed signal, Sig_0 was the thermal equilibrium magnetization, *TSL* was the time of spin-lock pulse, and *K* was the constant offset. The 2D T_2 images were calculated based on a similar expression: $Sig(TE) = Sig_0\exp(-TE/T_2)+K$, where *TE* was the echo time. Other experimental details have been described elsewhere (13,32).

Results

Images and depth-dependent profiles of T_2 and $T_{1\rho}$

Fig 1 and Fig 2 summarize the quantitative images and their depth-dependent profiles for four different types of specimens: native tissue (i.e., untreated), native tissue soaked in the Gd solution, trypsin-degraded tissue, and trypsin-degraded tissue soaked in the Gd solution.

Several distinct characteristics can be identified in these complex T_2 and $T_{1\rho}$ results at two different orientations (0° and 55° with respect to B_0). First, the tissue has clear laminar appearance in the T_2 and low spin-lock (0.5 kHz) $T_{1\rho}$ images at 0°, likely due to the strong influence of the dipolar interaction at 0° (the left column in Fig 2). Second, both T_2 and $T_{1\rho}$ at 55° are practically uniform (the right column in Fig 2), which is to be expected due to the minimization of the dipolar interaction at the magic angle. Third, even at 0°, the $T_{1\rho}$ images at 2 kHz are considerably uniform and have higher value, which signifies the minimization of the dipolar interaction by the high spin-lock field. Forth, regardless of the specimen orientation, T_2 at any tissue location always has the lowest value while $T_{1\rho}$ at higher spin-lock (2 kHz) always has the highest values (Fig 2). Among the $T_{1\rho}$ results, the larger the spin-lock field, the longer the $T_{1\rho}$ relaxation values, which is known as $T_{1\rho}$ dispersion.

The effects of trypsin digestion and Gd immersion

Two interesting features can be identified when the tissue is digested in trypsin or immersed in the Gd-DTPA^{2-} solution. First, the trypsin digestion causes the increase of T_2 and $T_{1\rho}$ over the entire tissue depth, regardless of whether the specimen is at 0° (Fig 2a vs Fig 2e) or 55° (Fig 2b vs Fig 2f). Second, for the native tissue, the soaking of specimen in the Gd solution does not change T_2 or $T_{1\rho}$ significantly (Fig 2a vs Fig 2c, and Fig 2b vs Fig 2d). However, the soaking of the degraded specimen in the Gd solution significantly reduces both T_2 and $T_{1\rho}$ (Fig 2e vs Fig 2g, and Fig 2f vs Fig 2h).

These variations in the T_2 and $T_{1\rho}$ profiles are quantified as the differences between the paired measurements in Fig 3, which have three depth-dependent characteristics. First, the T_2 difference is strongly depth-dependent at the 0° orientation - being mostly sensitive in the transitional zone (TZ) than at any other depth towards (1) the trypsin digestion (Fig 3a) and (2) the immersion of degraded tissue in Gd (Fig 3g). However, this T_2 difference in the transitional zone is significantly reduced when (1) both the native and degraded tissues have been immersed in Gd (Fig 3c) and (2) the native tissue is immersed in Gd (Fig 3e). Second, the weakly spin-locked $T_{1\rho}$ data (0.5 kHz) appears to have the similar characteristics as T_2, on a lesser scale. When the spin-lock filed is increased to 2 kHz, there is no obvious depth-dependence in $T_{1\rho}$ profiles. Third, both T_2 and $T_{1\rho}$ differences become somewhat depth-independent at the magic angle. In fact, all differences at the magic angle show a larger difference in the deeper part of the tissue than the surface part of the tissue (Fig 3b and 3h).

The zonal sensitivity of T_2 and $T_{1\rho}$ toward tissue degradation

Since most MRI studies of articular cartilage cannot achieve the fine spatial resolution as in this work (13–26 μm), the differences between the four paired experiments are averaged in each histological zone and plotted in two different ways (Fig 4): the percentage ratio and the absolute change. The division of zones was based on our knowledge of the tissue characteristics from the previous experiments – the nearly identical type of tissue has been studied in our lab for over 17 years by multidisciplinary imaging techniques at microscopic resolutions (33,34). In this project, the thicknesses of three structural zones were determined as, the superficial zone = 52 μm, the transitional zone = 78 μm, and the radial zone = 500 μm.

It was noticed that neither the percentage ratio nor the absolute change was a reliable indicator for the sensitivity of the measurement, due to two practical factors in the relaxation measurement, the influence of the experimental noises and the unreliability of low value relaxation measurement. For example, when a T_2 changed from 2 ms to 4 ms, it would be a 100% change. However, this 100% change at a low relaxation value of several milliseconds could contain a large error from the influence of experimental noises and the intrinsic unreliability of determining short relaxation times when the echo-time (TE) of an imaging

experiment is at least several milliseconds or longer. To better determine the sensitivity of the relaxation measurement, we define a term *Sensitivity*, which is given by,

$$\text{Sensitivity}=\text{Percentage}-\text{Ratio}\times\text{Absolute}-\text{Change} \quad (1),$$

, where the *Percentage-Ratio* is $(T_{after}-T_{before})/T_{before}$ in percentages, and the *Absolute-Change* is $(T_{after}-T_{before})$ in ms in this project. This quantity has the form of an equilateral hyperbola and can be plotted as a set of 2D contours, where each hyperbola equals a constant *Sensitivity*.

Fig 4 summarizes the zonal averaged Absolute-Change (ΔT), Percentage-Ratio (%) and Sensitivity (ms × %) in four sets of experimental conditions: (Fig 4a) degraded – native, (Fig 4b) degraded with Gd – degraded, (Fig 4c) native with Gd – native, and (Fig 4d) degraded with Gd – native with Gd. Several distinct features can be clearly identified. First, T_2 has sufficient sensitivity in all zones at 55° but only in TZ at 0° (Fig 4a) for the first and second sets of experimental comparisons. Second, $T_{1\rho}$ has sufficient sensitivity in all zones at both 0° and 55° for the first and second sets of experimental comparisons (Fig 4b). Neither T_2 nor $T_{1\rho}$ has sufficient sensitivity for the later two sets of experimental comparisons.

The trends of the individual sensitivities in the first and second sets of experimental comparisons can be visualized more clearly in a hyperbola contour plot (Fig 5), where the diagonal line points to an increasing *Sensitivity*. Any group of data points that are close together implies less variability in *Sensitivity*. Any data point (i.e., experimental condition) that is not near one of the axes or the origin is sensitive in the relaxation measurement. (For this reason, the data in Fig 4c and 4d are not plotted in Fig 5 since they all congregate near the origin.)

Discussion

In this study, high-resolution T_2 and $T_{1\rho}$ MRI experiments were carried out to study native and trypsin-degraded canine articular cartilage, at both the 0° and the magic angle. Several issues related to the measurement sensitivities of T_2 and $T_{1\rho}$ relaxation times towards cartilage degradation were investigated. These issues include (1) the characteristics of $T_{1\rho}$ dispersion (the value of $T_{1\rho}$ as the function of the spin-lock field), (2) the orientations of the specimen in the magnetic field B_0, (3) the PG content in tissue, and (4) the absence and presence of Gd ions in tissue. To better determine the usefulness of T_2 and $T_{1\rho}$ measurements in MRI diagnostics, a term *Sensitivity* is introduced in the data analysis, which includes the contributions from both the percentage changes and the absolute changes. We analyze the data in four different cases of experimental conditions: (Case a) the degradation of tissue without Gd ions (Fig 4a), (Case b) the degraded tissue without and with Gd ions (Fig 4b), (Case c) the native tissue without and with Gd ions (Fig 4c), and (Case d) the native and degraded tissues both in the presence of Gd ions (Fig 4d).

(Case a) Sensitivities of T_2 and $T_{1\rho}$ towards tissue degradation without the presence of Gd

T_2 is known to be sensitive to PG concentration and has been used in cartilage MRI (7,34–40). This report confirms the sensitivity of T_2 towards tissue degradation – T_2 increases when the PG content is reduced (Fig 4a). However, the sensitivity of MRI T_2 detection of cartilage lesion is both depth dependent and orientational dependent (Fig 4a), which is influenced by the dipolar interaction due to the anisotropic motion of water molecules associated with the collagen fibrils (7). This T2 anisotropy can therefore be used to explore the collagen structure in cartilage non-invasively. Since human joints never have any simple geometric shape, however, it is impossible to orient human in the magnet in such a way that the dipolar interaction has a uniform influence over the entire joint cartilage. Consequently,

although T_2 is a reliable marker in the research labs to study ex vivo tissue blocks (34), its sensitivity in human in vivo MRI depends on not only by the healthy status of cartilage but also by the orientation of cartilage in the MRI magnet. In comparison, the $T_{1\rho}$ sensitivity to tissue digestion is nearly uniform and isotropic, especially when the dipolar interaction is sufficiently minimized at the high spin-lock field (2 kHz). This makes the $T_{1\rho}$ protocol better suited for human MRI. However, a high spin-lock field increases the rf power deposition on the tissue, which is a distinct disadvantage in the $T_{1\rho}$ protocol when comparing with the T_2 protocol.

(Case b) Sensitivities of T_2 and $T_{1\rho}$ in degraded tissue without and with the presence of Gd ions

Gd ions diffuse into cartilage inversely to the local PG content in tissue: more into the PG-poor tissue region (e.g., SZ) and less into to PG-rich tissue region (e.g., RZ) (13). It is interesting to note that both T_2 and $T_{1\rho}$ are still very sensitive to the immersion of Gd ions in the degraded tissue (Fig 4b), which results in a set of sensitivity features similar to the degradation process in the absence of Gd ions (Fig 4a), including the strong depth-dependent T_2 sensitivity, the slightly depth-dependent $T_{1\rho}$ sensitivity at low spin-lock field, and the uniformly high $T_{1\rho}$ sensitivity at high spin lock field. The fact that T_2 at 0° is still depth-dependent demonstrates that the dipolar interaction still plays an important role in the relaxation process in the degraded tissue. The fact that T_2 at 55° is reduced (instead of increased) remarkably suggests the influx of additional paramagnetic Gd ions into the tissue, which dominates the relaxation process when the dipolar interaction is minimized (either at the magic angle or under the high spin-lock field). Our results are consistent with a human tissue MRI work by Taylor et al (30), with some interesting differences. For example, Taylor et al found that the addition of 1 mM Gd contrast agent shortened T_1 and $T_{1\rho}$ values significantly, but could not affect T2 values in articular cartilage. Additional investigation would be beneficial to identify the molecular mechanisms of these discrepancies.

(Case c) Sensitivities of T_2 and $T_{1\rho}$ in native tissue without and with the presence of Gd ions

When the native tissue is soaked in the Gd solution, however, both T_2 and $T_{1\rho}$ reduce slightly (Fig 4c). This result indicates that neither T_2 nor $T_{1\rho}$ has sufficient sensitivity to the presence of Gd ions in the native (i.e., healthy tissue with normal PG concentrations) tissue. This notable difference in the sensitivities of T_2 and $T_{1\rho}$ between the native tissue (Case c) with the degraded tissue (Case b) is a direct consequence of more PG in the native tissue, which limits the amount of Gd ions that can be diffused into the tissue.

(Case d) Sensitivities of T_2 and $T_{1\rho}$ in native and degraded tissue both in the presence of Gd ions

In the presence of the Gd ions, there are no significant differences in either T_2 or $T_{1\rho}$ between the native tissue and the degraded tissue (Fig 4d). This result reveals that the Gd ions largely eliminate the sensitivities of T_2 and $T_{1\rho}$ to PG degradation; in other words, the value of T_2 or $T_{1\rho}$ in the presence of Gd ions cannot be used as an indicator of a tissue's healthy status.

Sensitivities of T_2 and $T_{1\rho}$ at the magic angle

Since the profiles of T_2 and $T_{1\rho}$ at 55° are nearly depth-independent, these profiles were averaged over the entire tissue depth and presented in Fig 4 as one averaged value. However, the T_2 and $T_{1\rho}$ profiles at 55° clearly show that both T_2 and $T_{1\rho}$ also have some weak depth-dependent sensitivities at 55°, bout are more sensitive towards the deeper tissue (Fig 3a and 3h). This trend is likely caused by the non-uniform PG concentration in articular

cartilage – more PG at the deeper tissue (13). Hence there would be more PG loss at the deep tissue after the trypsin treatment, which results in more free water in deeper tissue and consequently a bigger difference in both T_2 and $T_{1\rho}$.

A potential clinical MRI protocol for tissue degradation by $T_{1\rho}$

It's interesting to note that $T_{1\rho}$ is more sensitive to the presence of Gd-DTPA^{2-} in PG-degraded specimens than in native specimens, i.e., the $T_{1\rho\text{-native}} - T_{1\rho\text{-native-Gd}}$ (Fig 4c) are much smaller than the $T_{1\rho\text{-degraded}} - T_{1\rho\text{-degraded-Gd}}$ (Fig 4b). This significant $T_{1\rho}$ difference between native specimens and trypsin-degraded specimens with and without the presence of Gd ions suggests a possible clinical protocol that can be very sensitive to the tissue degradation, that is, instead of examining the $T_{1\rho}$ values directly, one could do MRI $T_{1\rho}$ experiments, twice, with the second time in the presence of Gd ions. This double $T_{1\rho}$ procedure would be very similar to the current dGEMRIC procedure where T_1 of cartilage is imaged twice, with the second time in the presence of Gd ions. If there were little difference between the two $T_{1\rho}$ scans, the tissue would be healthy. More PG loss will result in a larger difference. Please note that the authors are not promoting a frequent use of the Gd ions in human MRI. This new protocol merely suggests that if Gd ions are being administrated into patients (like in the dGEMRIC protocol), then a double $T_{1\rho}$ protocol is more advantageous than a proper dGEMRIC protocol which requires two T_1 scans, since $T_{1\rho\text{-before}}$ has its own clinical significance (15,41) but $T_{1\text{-before}}$ does not (7). (Note that it is common in dGEMRIC to assume a constant $T_{1\text{-before}}$ and to acquire only the $T_{1\text{-after}}$ scan (42). However, considering the recent observation that $T_{1\text{-before}}$ and $T_{1\text{-after}}$ are both strain dependent (43), the assumption of a constant $T_{1\text{-before}}$ might be problematic if we need to consider the loading or loading history of the patient – the osteoarthritic cartilage is soft and, hence, easier to deform.)

It should be pointed that the high-resolution experiments in this project were performed at room temperature and a 7 Tesla magnet, which are somewhat different from the clinical conditions (1.5–3 Tesla and body temperature). Despite of its limitations in magnet size and other factors, μMRI is a perfect tool in the study of articular cartilage because of its ability to resolve fine tissue structures (tens of microns transversely) and its sensitivities to the delicate molecular environment. The developments at both microscopic and clinical resolutions should follow the resolution 'scaling law' in cartilage MRI (44), eventually leading to the successful diagnostics and management of cartilage lesion in human at its early stages.

Conclusions

In this microscopic imaging project, both T_2 and $T_{1\rho}$ relaxation times were studied in native and trypsin-degraded articular cartilage specimens, without and with the presence of 1 mM Gd-DTPA^{2-} and at both 0° and the magic angle. $T_{1\rho}$ values were very sensitive to PG loss regardless of the specimen orientation in the magnet field. The sensitivity of T_2 measurements to PG loss, by comparison, depended on the fibril orientation (more sensitive at the magic angle than at 0°) and the depth of cartilage (at 0°, more sensitive at TZ than SZ and RZ; at 55°, nearly uniform sensitivity). Compared to a slight decrement between native tissue with and without Gd solution, there was a more significant change between degraded tissue before/after soaked in Gd solution. The presence of 1 mM Gd-DTPA^{2-} reduced the sensitivity of both T_2 and $T_{1\rho}$ to cartilage degradation. However, a compound parameter, $T_{1\rho}$ without and with the presence of Gd-DTPA^{2-}, might become a sensitive parameter to detect the cartilage disease.

Acknowledgments

Yang Xia is grateful to the National Institutes of Health for the R01 grants (AR 045172 and AR 052353). The authors thank Drs. Mengjun Wang and Kefei Zhang in the Labs of Drs. C Les and H Sabbah (Henry Ford Hospital, Detroit) for helping the harvest of canine specimens, Ms Janelle Spann (Michigan Resonance Imaging, Rochester Hills, Michigan) for providing the contrast agent, and Ms Carol Searight (Oakland University) for editorial comments on the manuscript.

References

1. Maroudas A. Biophysical chemistry of cartilaginous tissues with special reference to solute and fluid transport. Biorheol. 1975; 12(3–4):233–248.
2. Venn M, Maroudas A. Chemical composition and swelling of normal and osteoarthritic femoral head cartilage. I. Chemical composition. Ann Rheum Dis. 1977; 36(2):121. [PubMed: 856064]
3. Buckwalter JA, Mankin HJ, Grodzinsky AJ. Articular cartilage and osteoarthritis. Instructional Course Lectures. 2005; 54:465. [PubMed: 15952258]
4. Kim DK, Ceckler TL, Hascall VC, Calabro A, Balaban RS. Analysis of water-macromolecule proton magnetization transfer in articular cartilage. Magn Reson Med. 1993; 29(2):211–215. [PubMed: 8429785]
5. Bacic G, Liu KJ, Goda F, Hoopes PJ, Rosen GM, Swartz HM. MRI contrast enhanced study of cartilage proteoglycan degradation in the rabbit knee. Magn Reson Med. 1997; 37(5):764–768. [PubMed: 9126951]
6. Gray ML, Burstein D, Xia Y. Biochemical (and functional) imaging of articular cartilage. Semin Musculoskelet Radiol. 2001; 5:329–344. [PubMed: 11745049]
7. Xia Y. Relaxation anisotropy in cartilage by NMR microscopy (μMRI) at 14μm resolution. Magn Reson Med. 1998; 39(6):941–949. [PubMed: 9621918]
8. Xia Y. Magic-angle effect in magnetic resonance imaging of articular cartilage: A review. Investigative Radiol. 2000; 35(10):602–621.
9. Mlynarik V, Mosher TJ, Smith HE, Dardzinski B. Magic angle effect in articular cartilage. Am J Roentgenol. 2002; 178(5):1287–1288. [PubMed: 11959749]
10. Bashir A, Gray ML, Burstein D. Gd-DTPA^{2-} as a measure of cartilage degradation. Magn Reson Med. 1996; 36(5):665–673. [PubMed: 8916016]
11. Burstein D, Velyvis J, Scott KT, Stock KW, Kim YJ, Jaramillo D, Boutin RD, Gray ML. Protocol issues for delayed Gd-DTPA^{2-} enhanced MRI (dGEMRIC) for clinical evaluation of articular cartilage. Magn Reson Med. 2001; 45(1):36–41. [PubMed: 11146483]
12. Tiderius CJ, Olsson LE, Leander P, Ekberg O, Dahlberg L. Delayed gadolinium-enhanced MRI of cartilage (dGEMRIC) in early knee osteoarthritis. Magn Reson Med. 2003; 49(3):488–492. [PubMed: 12594751]
13. Xia Y, Zheng SK, Bidthanapally A. Depth dependent profiles of glycosaminoglycans in articular cartilage by MRI and histochemistry. J Magn Reson Imaging. 2008; 28(1):151–157. [PubMed: 18581328]
14. Zheng SK, Xia Y. The impact of the relaxivity definition on the quantitative measurement of glycosaminoglycans in cartilage by the MRI dGEMRIC method. Magn Reson Med. 2010; 63(1): 25–32. [PubMed: 19918900]
15. Duvvuri U, Kudchodkar S, Reddy R, Leigh JS. T1ρ relaxation can assess longitudinal proteoglycan loss from articular cartilage in vitro. Osteoarthritis Cartilage. 2002; 10(11):838–844. [PubMed: 12435327]
16. Regatte RR, Akella SVS, Lonner JH, Kneeland JB, Reddy R. T1ρ relaxation mapping in human osteoarthritis (OA) cartilage: Comparison of T1ρ with T2. J Magn Reson Imaging. 2006; 23(4): 547–553. [PubMed: 16523468]
17. Bolbos RI, Link TM, Benjamin Ma C, Majumdar S, Li X. T1ρ relaxation time of the meniscus and its relationship with T1ρ of adjacent cartilage in knees with acute ACL injuries at 3 T. Osteoarthritis cartilage. 2009; 17(1):12–18. [PubMed: 18602280]

18. Li X, Pai A, Blumenkrantz G, Carballido-Gamio J, Link T, Ma B, Ries M, Majumdar S. Spatial distribution and relationship of T1ρ and T2 relaxation times in knee cartilage with osteoarthritis. Magn Reson Med. 2009; 61(6):1310–1318. [PubMed: 19319904]
19. Fullerton G, Cameron I, Ord V. Orientation of tendons in the magnetic field and its effect on T_2 relaxation times. Radiol. 1985; 155(2):433–435.
20. Peto S, Gillis P, Henri VP. Structure and dynamics of water in tendon from NMR relaxation measurements. Biophys J. 1990; 57(1):71–84. [PubMed: 2297563]
21. Xia Y, Farquhar T, Burton-Wurster N, Lust G. Origin of cartilage laminae in MRI. J Magn Reson Imaging. 1997; 7(5):887–894. [PubMed: 9307916]
22. Bashir A, Gray ML, Hartke J, Burstein D. Nondestructive imaging of human cartilage glycosaminoglycan concentration by MRI. Magn Reson Med. 1999; 41(5):857–865. [PubMed: 10332865]
23. Virta A, Komu M, Kormano M. $T_{1\rho}$ of protein solutions at very low fields: dependence on molecular weight, concentration, and structure. Magn Reson Med. 1997; 37(1):53–57. [PubMed: 8978632]
24. Duvvuri U, Goldberg AD, Kranz JK, Hoang L, Reddy R, Wehrli FW, Wand AJ, Englander S, Leigh JS. Water magnetic relaxation dispersion in biological systems: the contribution of proton exchange and implications for the noninvasive detection of cartilage degradation. Proceedings Nat Acad Sci USA. 2001; 98(22):12479–12484.
25. Li X, Han ET, Busse RF, Majumdar S. In vivo T1ρ mapping in cartilage using 3D magnetization-prepared angle-modulated partitioned *k*-space spoiled gradient echo snapshots (3D MAPSS). Magn Reson Med. 2008; 59(2):298–307. [PubMed: 18228578]
26. Akella SVS, Regatte RR, Wheaton AJ, Borthakur A, Reddy R. Reduction of residual dipolar interaction in cartilage by spin-lock technique. Magn Reson Med. 2004; 52(5):1103–1109. [PubMed: 15508163]
27. Stanisz GJ, Henkelman RM. Gd-DTPA relaxivity depends on macromolecular content. Magn Reson Med. 2000; 44(5):665–667. [PubMed: 11064398]
28. Henkelman RM, Stanisz GJ, Menezes N, Burstein D. Can MTR be used to assess cartilage in the presence of Gd-DTPA^{2-}? Magn Reson Med. 2002; 48(6):1081–1084. [PubMed: 12465122]
29. Nieminen MT, Menezes NM, Williams A, Burstein D. T2 of articular cartilage in the presence of Gd-DTPA^{2-}. Magn Reson Med. 2004; 51(6):1147–1152. [PubMed: 15170834]
30. Taylor C, Carballido-Gamio J, Majumdar S, Li X. Comparison of quantitative imaging of cartilage for osteoarthritis: T2, T1ρ, dGEMRIC and contrast-enhanced computed tomography. Magn Reson Imaging. 2009; 27(6):779–784. [PubMed: 19269769]
31. Xia Y, Farquhar T, Burton-Wurster N, Vernier-Singer M, Lust G, Jelinski L. Self-diffusion monitors degraded cartilage. Arch Biochem Biophys. 1995; 323(2):323–328. [PubMed: 7487094]
32. Zheng SK, Xia Y, Bidthanapally A, Badar F, Ilsar I, Duvoisin N. Damages to the extracellular matrix in articular cartilage due to cryopreservation by microscopic magnetic resonance imaging and biochemistry. Magn Reson Imaging. 2009; 27(5):648–655. [PubMed: 19106023]
33. Xia Y, Moody J, Burton-Wurster N, Lust G. Quantitative In Situ Correlation Between Microscopic MRI and Polarized Light Microscopy Studies of Articular Cartilage. Osteoarthritis Cartilage. 2001; 9(5):393–406. [PubMed: 11467887]
34. Alhadlaq H, Xia Y, Moody JB, Matyas J. Detecting Structural Changes in Early Experimental Osteoarthritis of Tibial Cartilage by Microscopic MRI and Polarized Light Microscopy. Ann Rheum Dis. 2004; 63(6):709–717. [PubMed: 15140779]
35. Mosher TJ, Smith H, Dardzinski BJ, Schmithorst VJ, Smith MB. MR imaging and T2 mapping of femoral cartilage: in vivo determination of the magic angle effect. Am J Roentgenol. 2001; 177(3): 665–669. [PubMed: 11517068]
36. Menezes NM, Gray ML, Hartke JR, Burstein D. T2 and T1ρ MRI in articular cartilage systems. Magn Reson Med. 2004; 51(3):503–509. [PubMed: 15004791]
37. Trattnig S, Millington SA, Szomolanyi P, Marlovits S. MR imaging of osteochondral grafts and autologous chondrocyte implantation. Eur Radiol. 2007; 17(1):103–118. [PubMed: 16802126]

38. Watanabe A, Boesch C, Siebenrock K, Obata T, Anderson SE. T2 mapping of hip articular cartilage in healthy volunteers at 3T: a study of topographic variation. J Magn Reson Imaging. 2007; 26(1):165–171. [PubMed: 17659572]

39. Nissi MJ, Rieppo J, Toyras J, Laasanen MS, Kiviranta I, Nieminen MT, Jurvelin JS. Estimation of mechanical properties of articular cartilage with MRI - dGEMRIC, T2 and T1 imaging in different species with variable stages of maturation. Osteoarthritis Cartilage. 2007; 15(10):1141–1148. [PubMed: 17513137]

40. Zheng S, Xia Y. Multi-components of T2 relaxation in ex vivo cartilage and tendon. J Magn Reson. 2009; 198(2):188–196. [PubMed: 19269868]

41. Regatte RR, Akella SVS, Borthakur A, Kneeland JB, Reddy R. Proteoglycan Depletion-Induced Changes in Transverse Relaxation Maps of Cartilage: Comparison of T2 and T1ρ. Acad Radiol. 2002; 9(12):1388–1394. [PubMed: 12553350]

42. Kim YJ, Jaramillo D, Millis MB, Gray ML, Burstein D. Assessment of early osteoarthritis in hip dysplasia with delayed gadolinium-enhanced magnetic resonance imaging of cartilage. J Bone Joint Surg. 2003; 85A(10):1987–1992. [PubMed: 14563809]

43. Xia Y, Wang N, Lee J, Badar F. Strain-dependent T1 relaxation profiles in articular cartilage by MRI at microscopic resolutions. Magn Reson Med. 2011; 65:1733–1737. [PubMed: 21452280]

44. Xia Y. Resolution 'scaling law' in MRI of articular cartilage. Osteoarthritis Cartilage. 2007; 15(4): 363–365. [PubMed: 17218119]

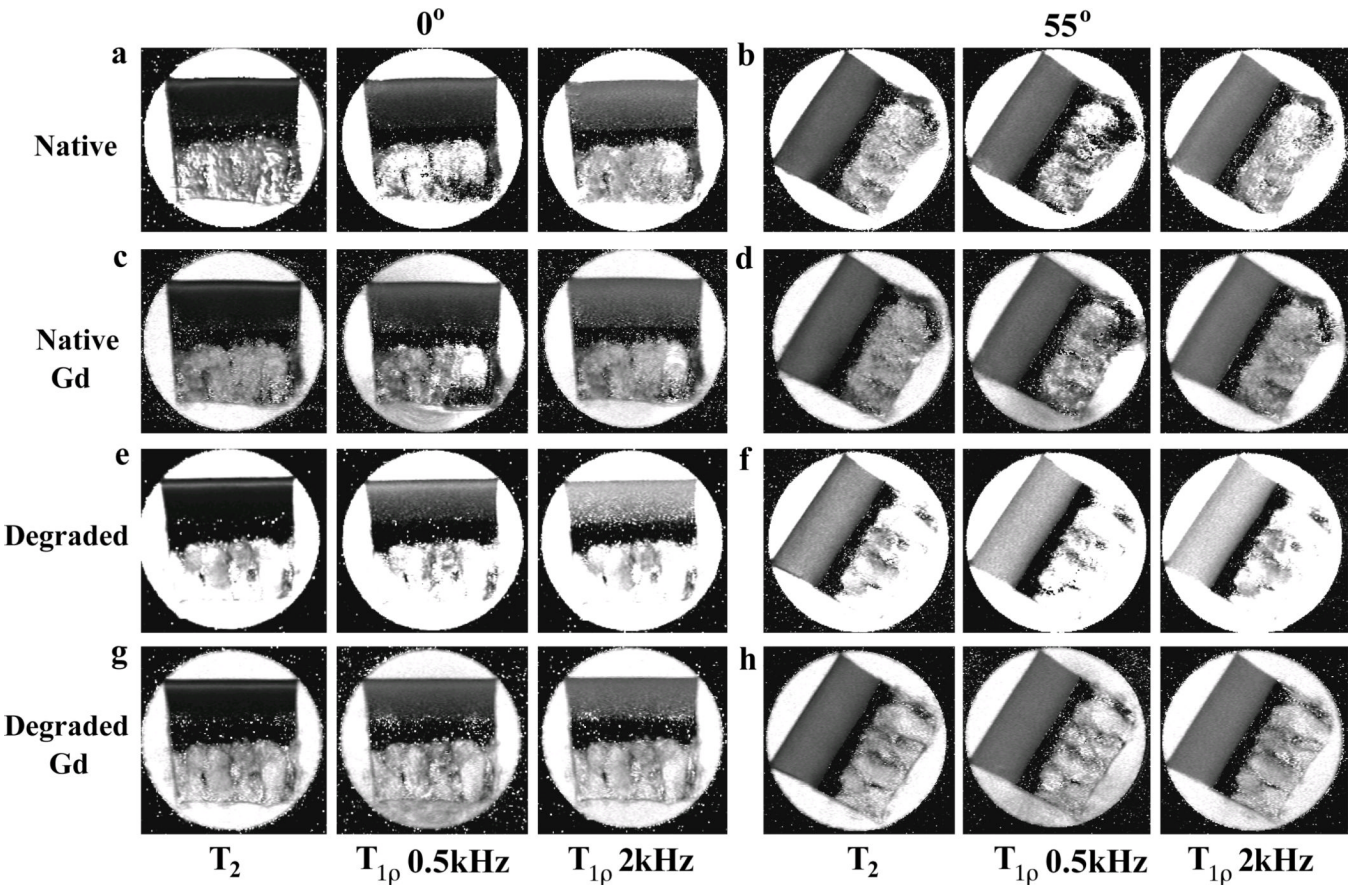

Figure 1.

T_2 and $T_{1\rho}$ images at four sets of experimental conditions: (a–b) native specimens, (c–d) native specimens immersed in Gd-DTPA^{2-}, (e–f) trypsin-degraded specimens, (g–h) trypsin-degraded specimens immersed in Gd-DTPA^{2-}. All images were plotted with the same intensity limits (0 – 200 ms). The angles 0° (left) and 55° (right) refer to the orientation between the normal axis of the surface and the magnetic field (vertically up).

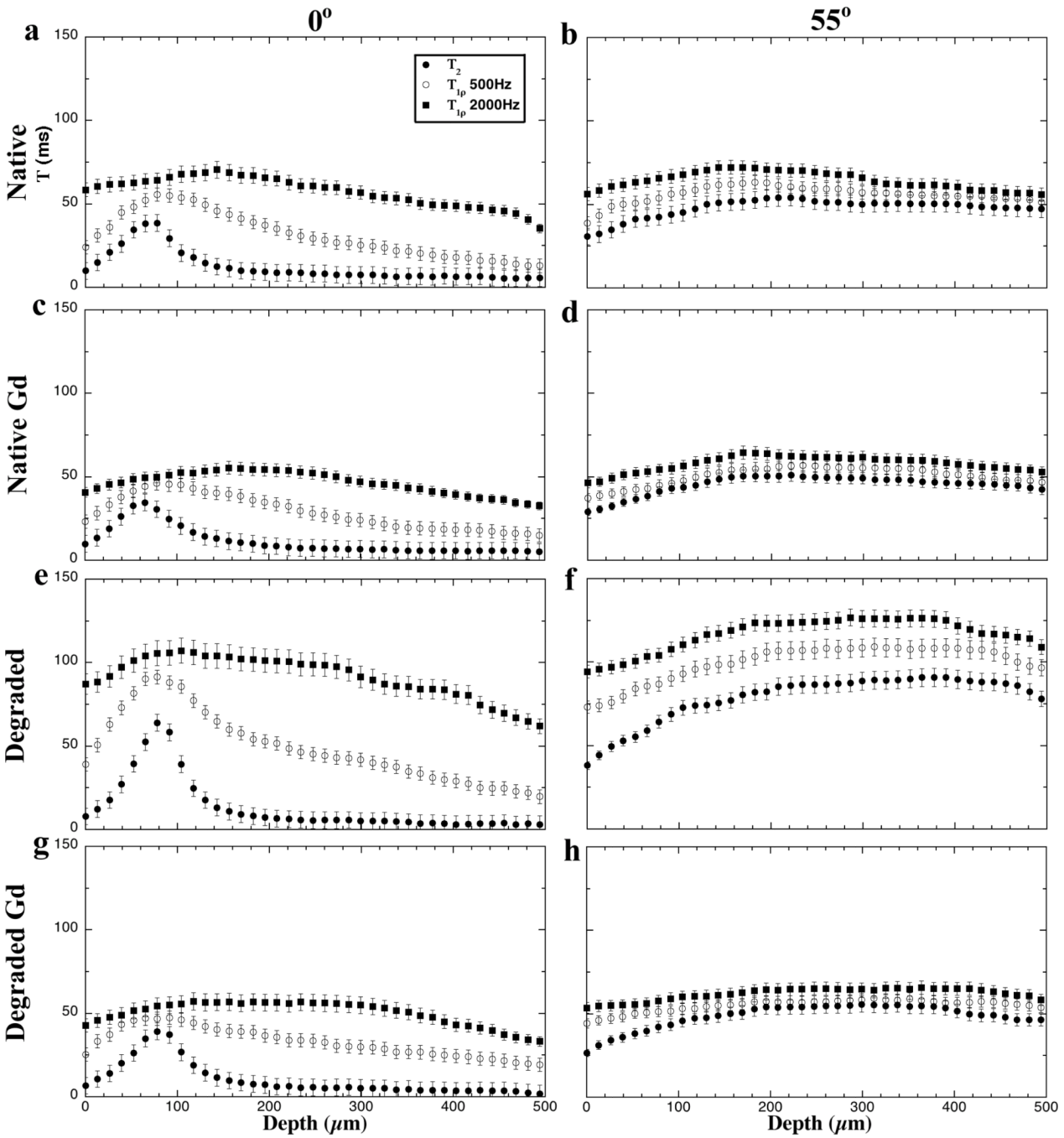

Figure 2.

T_2 and $T_{1\rho}$ profiles of articular cartilage at four experimental conditions, at 0° (left) and 55° (right). All profiles were plotted with the same intensity limits (0 – 150 ms).

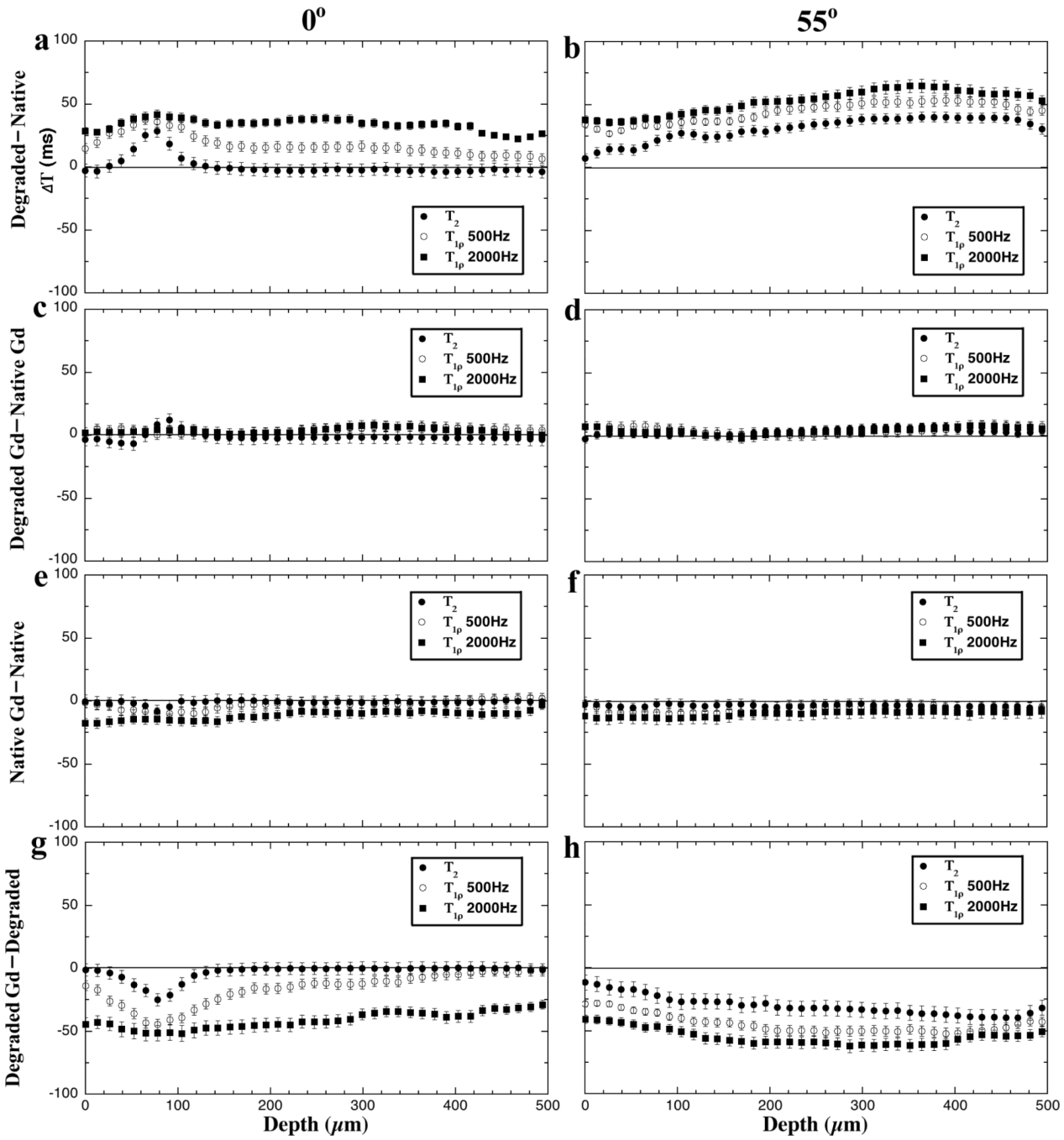

Figure 3.
The difference profiles of T_2 and $T_{1\rho}$ at 0° (left) and 55° (right) at four sets of comparisons.

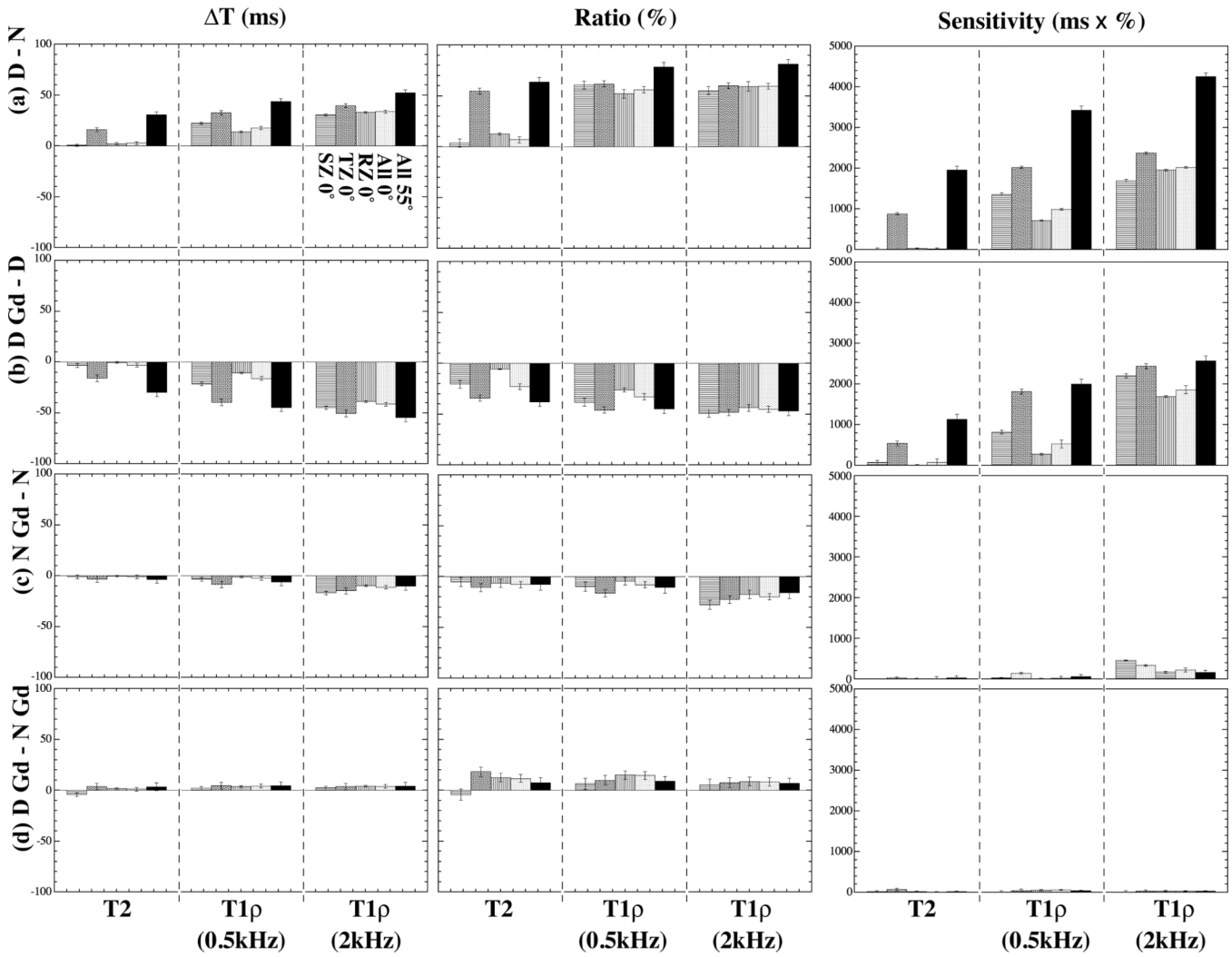

Figure 4.

The zonal averaged differences of T_2 and $T_{1\rho}$ at 0° and 55°. The left column: the difference of relaxation measurement (ΔT in ms); the middle column: the percentage ratio of relaxation measurement (%); the right column: the sensitivity of relaxation measurement (ms × %). (a) – (d) correspond to the four sets of comparisons shown in Fig 3.

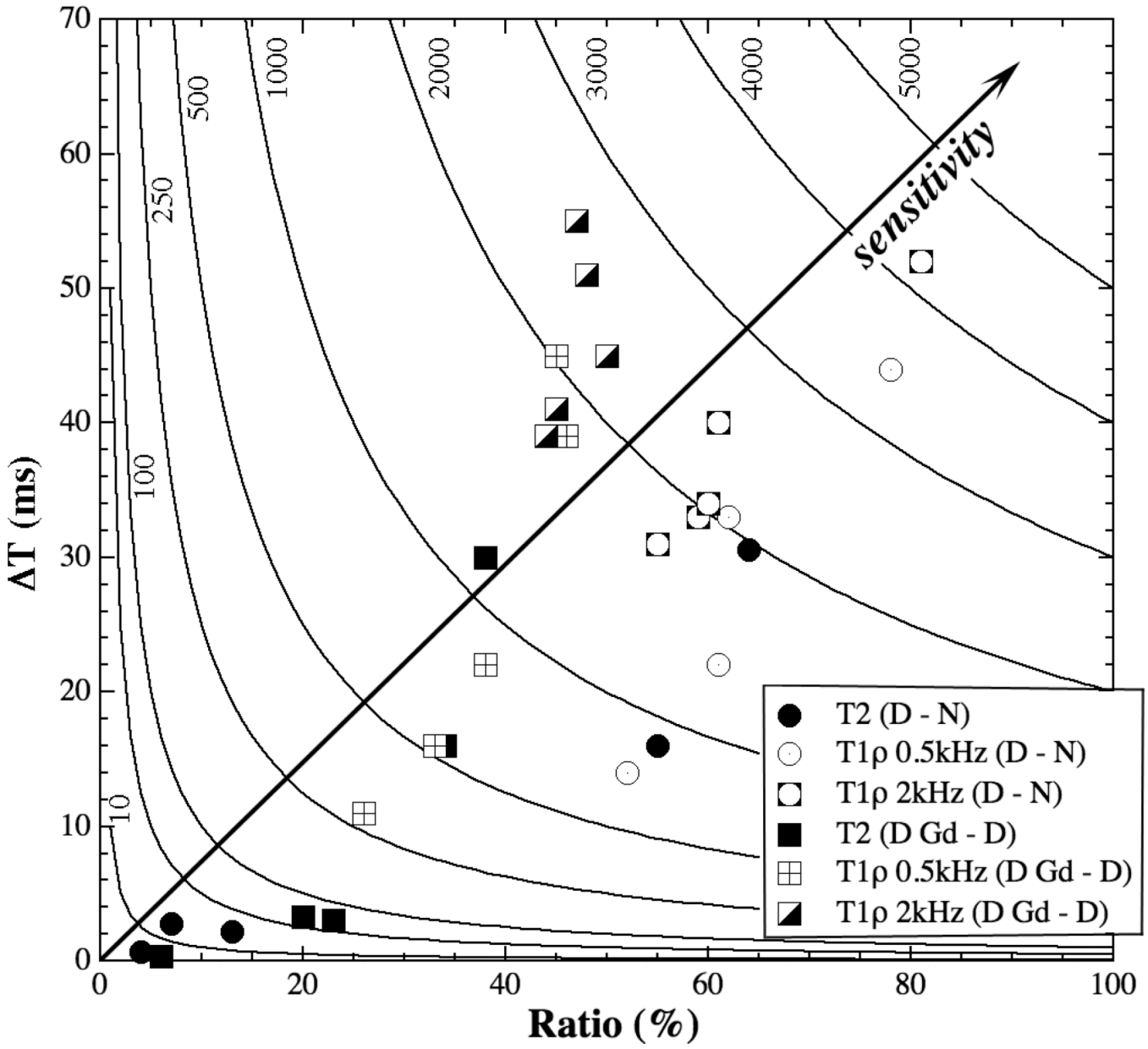

Figure 5.
The sensitivities in the first and second sets of comparisons in a hyperbola contour, where the diagonal arrow line points to an increasing *Sensitivity*.